Supplementary Information

Continuous-Flow Reactor with Superior Production Rate and Stability for CO_2 reduction using Semiconductor Photocatalysts

Hyunju Jung[1,2], Chansol Kim[3], Hae-Wook Yoo[4], Jei You[5], Jin Seog Kim[5], Aqil Jamal[6], Issam Gereige[6], Joel W. Ager[2, 7]*, and Hee-Tae Jung[1, 8]*

[1] Department of Chemical and Biomolecular Engineering, Korea Advanced Institute of Science and Technology (KAIST), 291 Daehak-ro, Yuseong-gu, Daejeon 34141, South Korea

[2] Chemical Sciences Division, Lawrence Berkeley National Laboratory, 1 Cyclotron Road, Berkeley, California 94720, USA

[3] Clean Energy Research Center, Korea Institute of Science and Technology (KIST), Hwarang-ro 14-gil 5, Seongbuk-gu, 02792, South Korea

[4] The First R&D Institute, Agency for Defense Development, Yuseong-gu, Daejeon 305-600, South Korea

[5] Gas Isotope Metrology Team, Korea Research Institute of Standards and Science, Daejeon 34113, South Korea

[6] Saudi Aramco, Research and Development Center, Dhahran, 31311 Saudi Arabia

[7] Department of Materials Science and Engineering, University of California Berkeley

[8] Korea Advanced Institute of Science and Technology (KAIST) Institute for Nanocentury, Daejeon 34141, South Korea

*Corresponding author. Email: jwager@lbl.gov, heetae@kaist.ac.kr

This file includes:

Materials and Methods

Materials

Methanol (MeOH), Nafion 117 solution (~5 wt%), chloroplatinic acid solution (H_2PtCl_6, 8 wt% in H_2O), zinc oxide (ZnO), and cadmium sulfide (CdS) were purchased from Sigma-Aldrich. TiO_2 powder (P25, Degussa) and C_3N_4 powder were used as received. The gas diffusion layer (GDL; Porex PM21M) was purchased from Fuel Cell Store. All chemicals were used as received without further purification.

Preparation of catalyst layers

The catalyst ink applied to all of the photocatalytic materials in this work was prepared through the ultrasonic dispersion of 10 mg of the catalyst powder with 20 μL of Nafion solution in 10 mL MeOH for 30 min. Then, 500 μL of the as-prepared catalyst ink was spray-coated on the GDL, and the electrode was dried overnight.

Synthesis of Pt-P25

The Pt-P25 photocatalysts were prepared through a photoreduction method. In a typical process [1,2], 1 g of P25 powder was suspended in a 100 mL solution (H_2O:MeOH = 7:3 v/v). Then, 5 mg of the H_2PtCl_6 solution (0.5 wt%) was added into the suspension under ultrasonication and stirred in the dark for 3 h before irradiation under a 300 W Xe lamp for 3 h. The obtained products were washed, filtered, and dried overnight at 80 °C. Finally, Pt-P25 powder was applied to GDL in the same manner as described above and used in the experiment.

Photocatalytic reaction in batch reactors

For the gas-phase batch reaction, the test for photocatalytic CO_2 conversion performance was conducted in a 50 mL SUS reactor with a quartz window on the top. The light source was a 300 W Xe lamp, and the intensity of light in the reactor was 300 mW/cm^2. A 1 cm^2 specimen of the sample was placed at the bottom of the reactor, and the vessel was charged with 4 mL of H_2O. The reactor was sufficiently purged with CO_2 to ensure that the catalyst was saturated with CO_2 and H_2O vapors.

For the liquid-phase batch reaction, the experiment was performed under the same conditions as those used for the gas-phase reaction, but a 96 mL glass reactor with a quartz window filled with 50 mL of CO_2 purged water was used. Photocatalytic reactions were allowed to occur for each set time, and the amounts of the CO and CH_4 obtained were analyzed using a gas chromatograph (GC; Agilent 7890GC) connected to the reactor.

Photocatalytic reaction in the photo-GDE

The custom-made photo-GDE shown in Fig. S1 was built in-house and consists of a quartz window housing, gaskets, a catalyst layer, a gas flow plate, an electrolyte flow plate, and a back plate. The window housing, flow plates, and back plate were made from stainless steel, owing to its chemical inertness, with sizes of 6×6×1 cm^3. Pressurized gas flow was controlled using a gas regulator and a mass flow meter, and transported to gas flow plate adjoining one side of the catalyst layer through a ⅛″ diameter Teflon-lined tube. The electrolyte plate was filled with water cycled by a peristaltic pump and the electrolyte feed was delivered to the other side of the catalyst layer through a ⅛″ diameter Teflon tube. Light from a 300 W Xe lamp passed through the window housing and the electrolyte to the catalyst layer surface. All gaskets and flow plates had a 1 cm^2 hole in the middle. All parts were assembled and fastened with four bolts. The product generated by the continuous reaction under light irradiation entered the in-

line GC system for analysis during each of the set reaction times. Before measurement, the baseline was checked by measuring pure CO_2 gas to detect any residual gas in the reactors.

Isotope-labeling measurement

The isotope-labeling test was conducted using $^{13}CO_2$ (isotope purity 99% < 2% ^{18}O and chemical purity 99.8%; Cambridge Isotope Laboratories, Inc.) as the carbon source. For accurate measurements, the reaction was allowed to occur under high-concentration conditions: gas flow rate of 2 sccm, gas pressure of 1.2 bar, and water flow rate of ~166 mL/min. Other conditions for $^{13}CO_2$ photoreduction were the same as those utilized for other photoreactions in the flow system. The gas products were analyzed by gas chromatography–mass spectrometry (7890B GC Agilent Technologies, USA, 5977A Series GC/MSD System, Agilent Technologies, USA) equipped with a column for detecting $^{13}CH_4$ and ^{13}CO products (RT-MOLESIEVE 13 X, 30 m × 0.21 mm × 30 μm). Helium was used as the carrier gas at a flow rate of 2 mL/min.

Product analysis

The production rate in the batch-type reactor was determined according to the following equations:

For the CO production rate:

$$y_{CO} = \frac{CO\ produced\ (mol)}{catalyst\ amount\ (g) \cdot reation\ time\ (hr)}$$

$$= \frac{fraction\ of\ CO\ (\%) \cdot Reactor\ Pressure\ (atm) \cdot Reactor\ volume\ (L)}{0.082\left(\frac{atm \cdot L}{mol \cdot K}\right) \cdot reactor\ Tempaerature\ (K) \cdot catalyst\ amount\ (g) \cdot reation\ time\ (hr)}.$$

In the case of a flow reactor such as photo-GDE, the production rate was calculated by considering the total number of moles of gas entering the GC system and the ratio of the products formed therein.

For the CO production rate:

$$y_{CO} = \frac{CO\ produced\ (mol)}{catalyst\ amount\ (g) \cdot reation\ time\ (hr)} = \frac{fraction\ of\ CO\ (\%) \cdot n_{total}}{catalyst\ amount\ (g) \cdot reation\ time\ (hr)}$$ and

$$n_{total} = \frac{\frac{atmospheric\ pressure\ (atm) \cdot injected\ sample\ volume\ (L)}{0.082\left(\frac{atm \cdot L}{mol \cdot K}\right) \cdot room\ temperature\ (K)}}{}$$

$$= \frac{atmospheric\ pressure \cdot gas\ flow\ rate\left(\frac{ml}{min}\right) \cdot gas\ flow\ time\ (min)}{0.082\left(\frac{atm \cdot L}{mol \cdot K}\right) \cdot room\ temperature\ (K)}.$$

By combining the above two formulas, as the reaction time was the same as the time of the gas flow in a continuous reactor:

$$y_{co} = \frac{fraction\ of\ CO\ (\%) \cdot atmospheric\ pressure \cdot gas\ flow\ rate\left(\frac{ml}{min}\right)}{0.082\left(\frac{atm \cdot L}{mol \cdot K}\right) \cdot room\ temperature\ (K) \cdot catalyst\ amount\ (g)}.$$

The production rate of CH_4 was determined in the same manner as shown above.

Table S1. The process and factors for stabilizing the system. The critical factors: 1) Light direction, 2) gas flow control under pressurized 3) water flow control.

Process	Issues	Solutions	Factor
Stability of system	Carbon-based GDLs are easily damaged during the reaction.	In the photocatalytic reaction, conductive support is not essential, so robust and thin PTFE GDL is used.	Robust support materials for GDL
Light Direction	GDL is opacity	Irradiate light towards the catalyst coated side	light irradiation on the catalyst
	When light irradiated through gas layer, water does not encounter the catalyst through GLD	Irradiate light through a quartz window filled with water.	Supply all reactants to the catalyst
Temperature control	The temperature rise is large by heating the water trapped in the light.	Electrolyte converted to flow form with an open bottle.	Distributes heat build-up with fluid flow
Water line configuration	At pressures above atmospheric pressure, the gas escapes as bubbles towards the water layer.	Connect both sides of the water line to circulate in a closed state.	Pressure equalization with closed water line
Water flow rate control	As the water circulation rate increases, water overflows into the gas layer.	Equilibrate by increasing the pressure or lowering the water flow rate	Appropriate water flow rate range
Gas flow control.	Gas with pressure cannot flow into the reactor with a constant flow rate. Flow control through the MFC does not vent pressurized gas.	The pressure in the gas line going into the reactor is regulated and the outgoing gas is passed through the MFC to control the flow rate.	Simultaneously control the pressure at the front of the reactor and the flow rate at the rear
	Moisture permeates the MFC, making it difficult to control accurately	The gas flow rate exiting the reactor is controlled through the needle valve, and it is accurately measured by MFM after the gas exiting through the GC.	Stable and precise flow control with mechanical valves and digital meters
	At high gas pressure, gas leaks as bubbles into the electrolyte layer	Adjust the pressure range until gas comes out of the bubble.	Appropriate gas pressure range

Table S2. The photocatalytic performances of P25 in CO_2 reduction reaction.

Reactor type	Reactant supply	Reaction time	Light source	Production rate	Ref. No.
Continuous flow reactor	CO_2 gas diffused into photocatalyst layer and water flowed in front of catalyst layer	720 min	300W Xe lamp	CO: 327 μmol/g·hr CH_4: 23.6 μmol/g·hr	This work
Liquid Batch cell	CO_2 purged water	240 min	300W Xe lamp	CO: 0.5 μmol/g·hr	[3]
Gas Batch cell	CO_2 gas purged to reactor with D.I water	60min	300W Xe lamp	CO: 1.7 μmol/g·hr CH_4: 0.42 μmol/g·hr	[4]
Gas Batch cell	Humidified CO_2 gas	360min	1 Sun Solar simulator with 425nm cutoff filter	CO: 0.5 μmol/g·hr	[5]
Gas Batch cell	CO_2 gas purged to reactor with D.I water	180min	300W Xe lamp	CO: 3.97 μmol/g·hr CH_4: 0.06 μmol/g·hr	[6]
Gas Batch cell	CO_2 gas purged to reactor with D.I water	600min	300W Xe lamp	CO: 3.54 μmol/g·hr CH_4: 0.02 μmol/g·hr	[7]
Gas Batch cell	CO_2 gas purged to reactor with D.I water	300min	300W Xe lamp	CO: 0.39 μmol/g·hr CH_4: 0.1 μmol/g·hr	[8]
Liquid Batch cell	CO_2 purged water	360min	high-pressure Hg lamp	CH_4: 4 μmol/g·hr	[9]

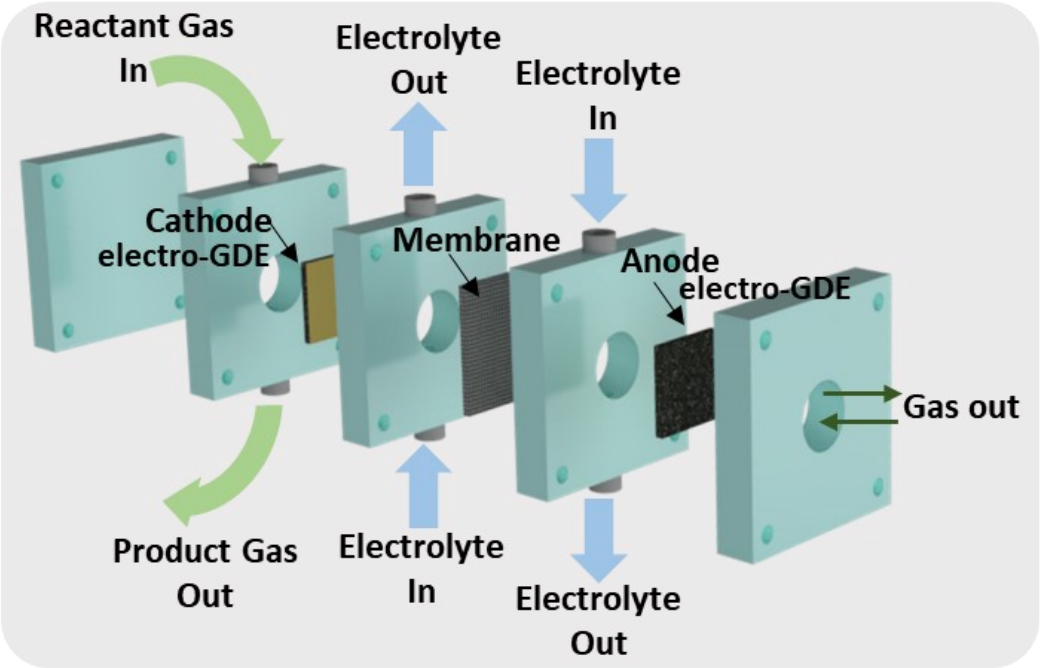

Figure S1. Magnified diagram of a conventional electro-GDE system.

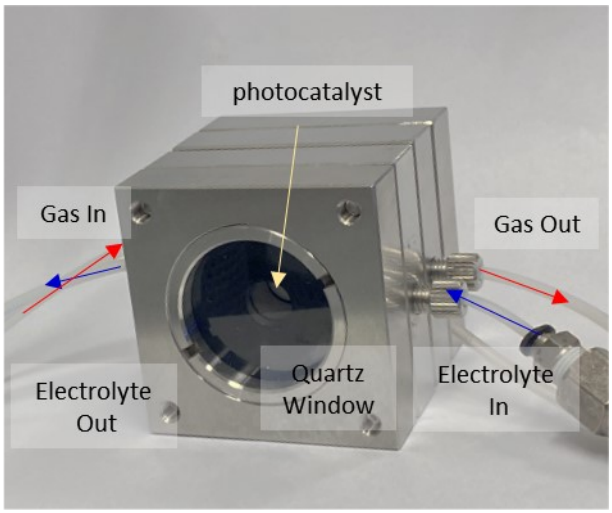

Figure S2. Photograph of the assembled continuous-flow photocatalytic reactor.

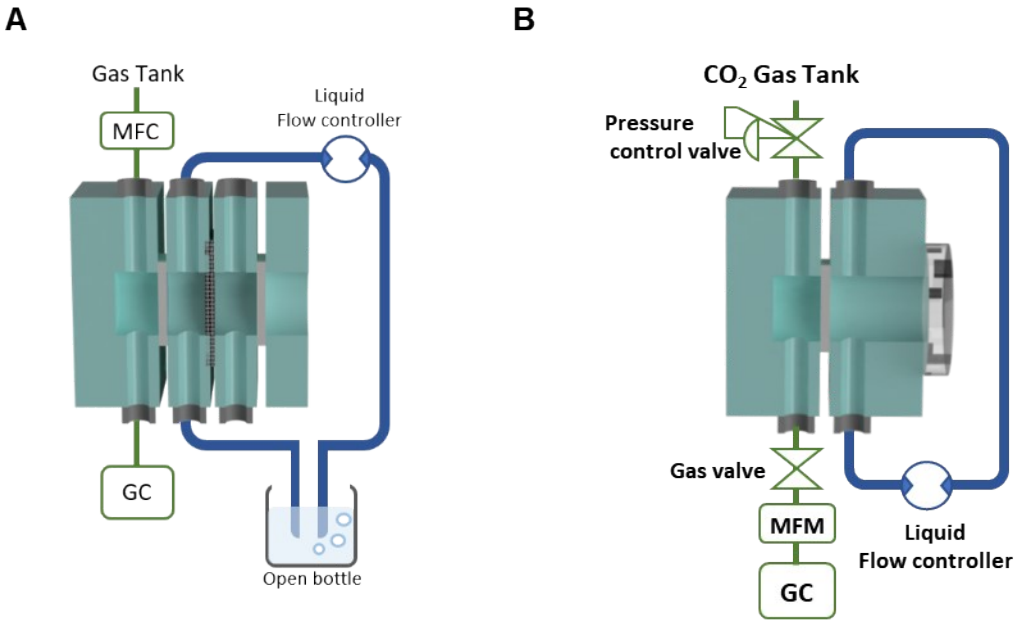

Figure S3. Schematic of the system connections of (A) the flow system of the electrocatalytic system and (B) the continuous-flow photocatalytic reactor system.

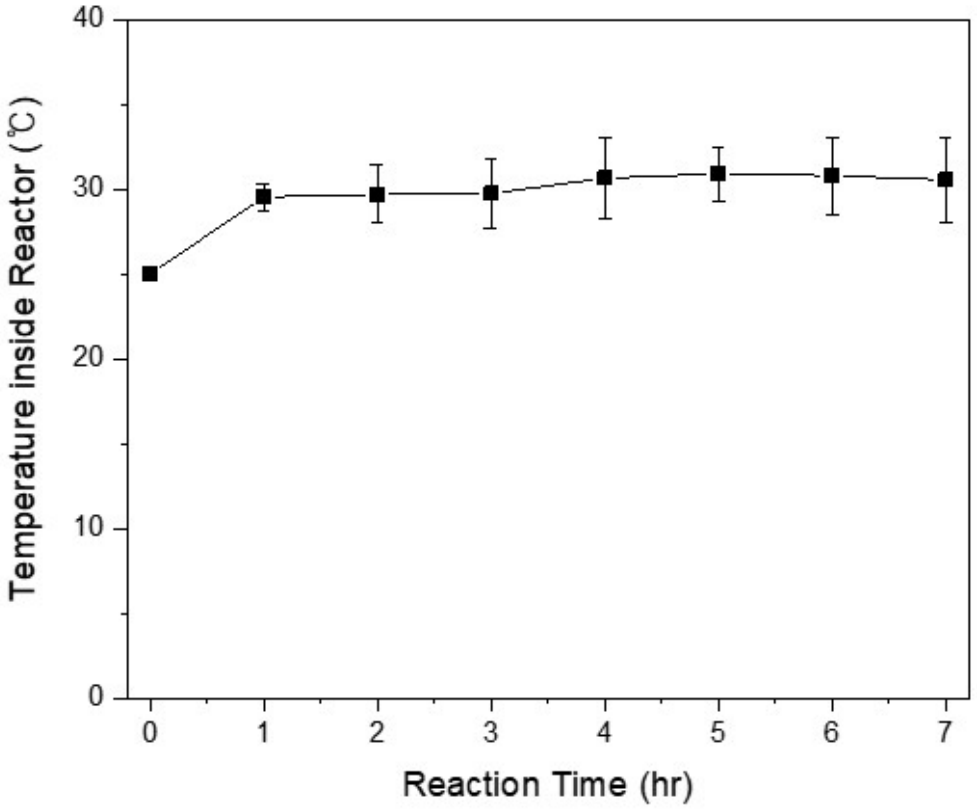

Figure S4. Internal temperature of the reactor as a function of reaction time. Real-time temperature measurements were conducted by inserting a thermocouple inside the liquid plate. Even if the reaction proceeded for greater than 7 h, the temperature inside the reactor did not exceed ~ 30℃.

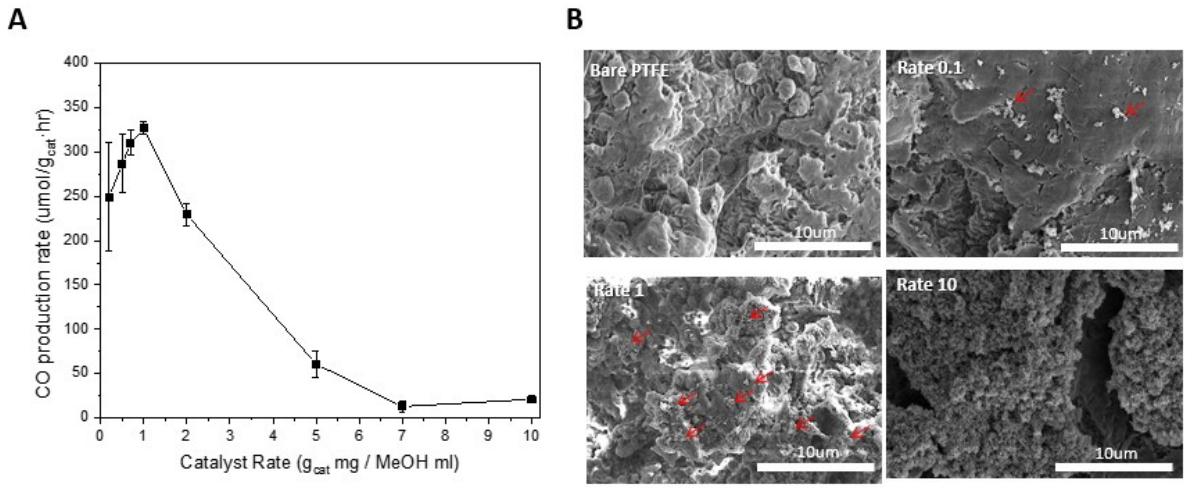

Figure S5. CO production rate and dispersed catalyst images as a function of the catalyst loading amounts. (**A**) CO production rates with various catalyst loading amounts. The catalyst rate was calculated by dividing the volume of methanol solvent by the amount of catalyst in the catalyst ink. The same volume of catalyst inks (500 μL) was applied to the PTFE film. (**B**) Surface images from scanning electron microscopy (SEM) according to each of the loading amounts: bare PTFE film, catalyst rates of 0.1, 1, and 10 mg/mL.

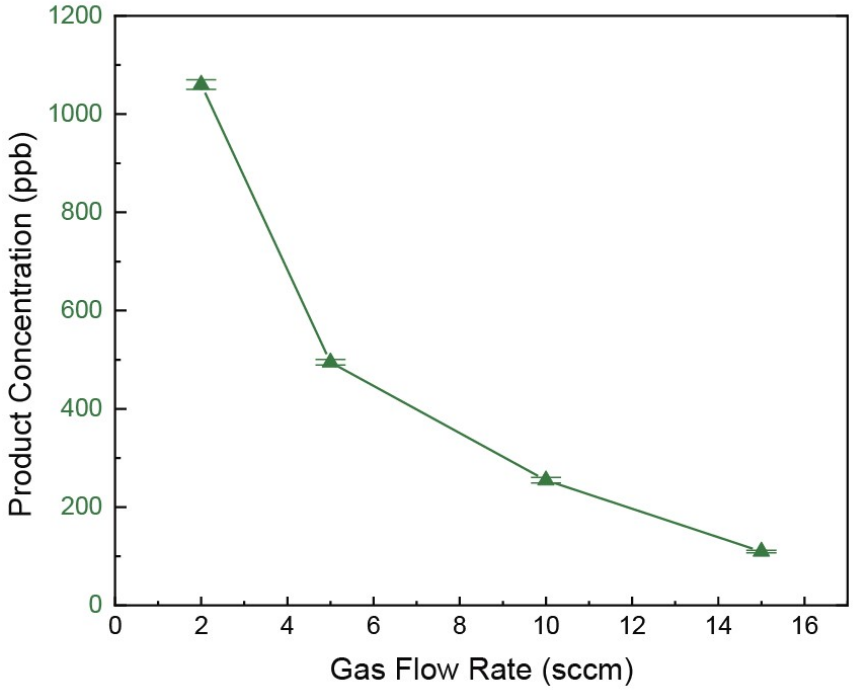

Figure S6. Product concentration as a function of the gas flow rate in the photocatalytic flow reactor system in this work under same reaction conditions: P25 (rate 1) on PTFE, 300W Xe Lamp irradiation, CO_2 gas pressure: 1.2 bar, electrolyte flow rate: 16.6 mL/min.

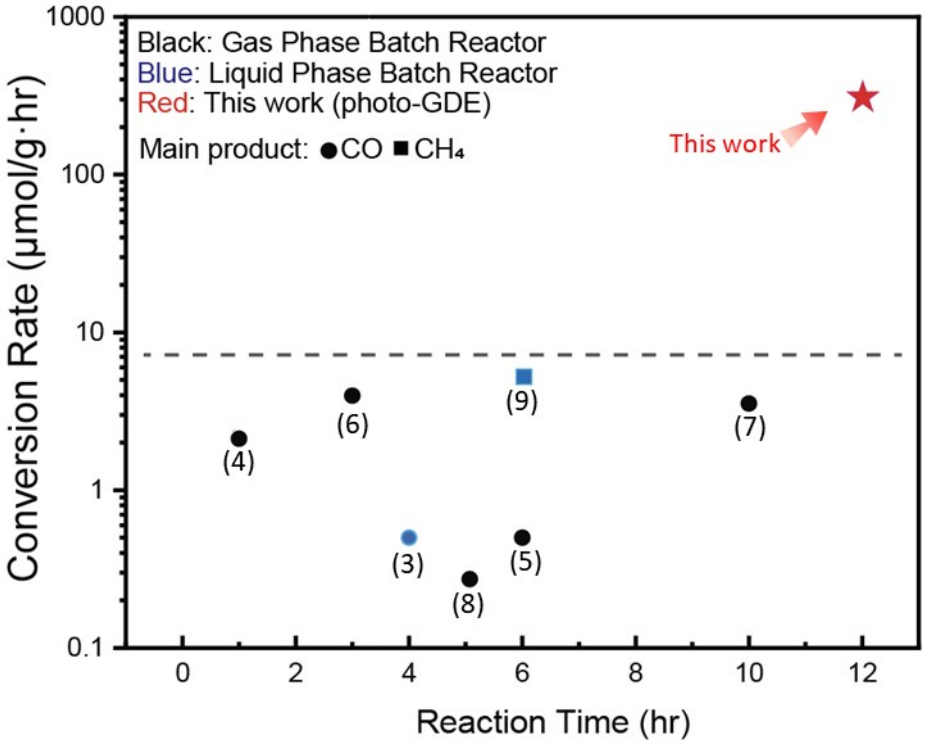

Figure S7. State-of-the-art CO_2 photoconversion rates of P25. Conversion rates of CH_4 (solid square, ■) and CO (empty circle, ○) for CRR photocatalysts as a function of reaction time.[3–9]

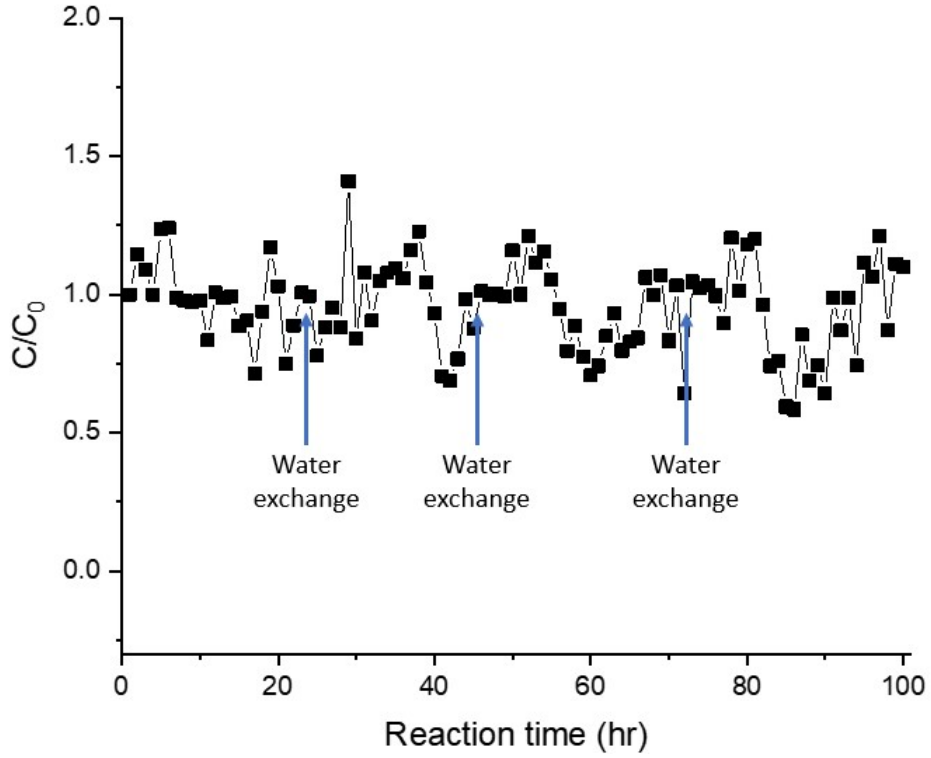

Figure S8. **Ratio of the total production rate to the initial value (C/C_0) measured in the flow-type photocatalytic reactor in 100hr.** Water lost due to evaporation was replenished every 24 hours (indicated by the blue arrow).

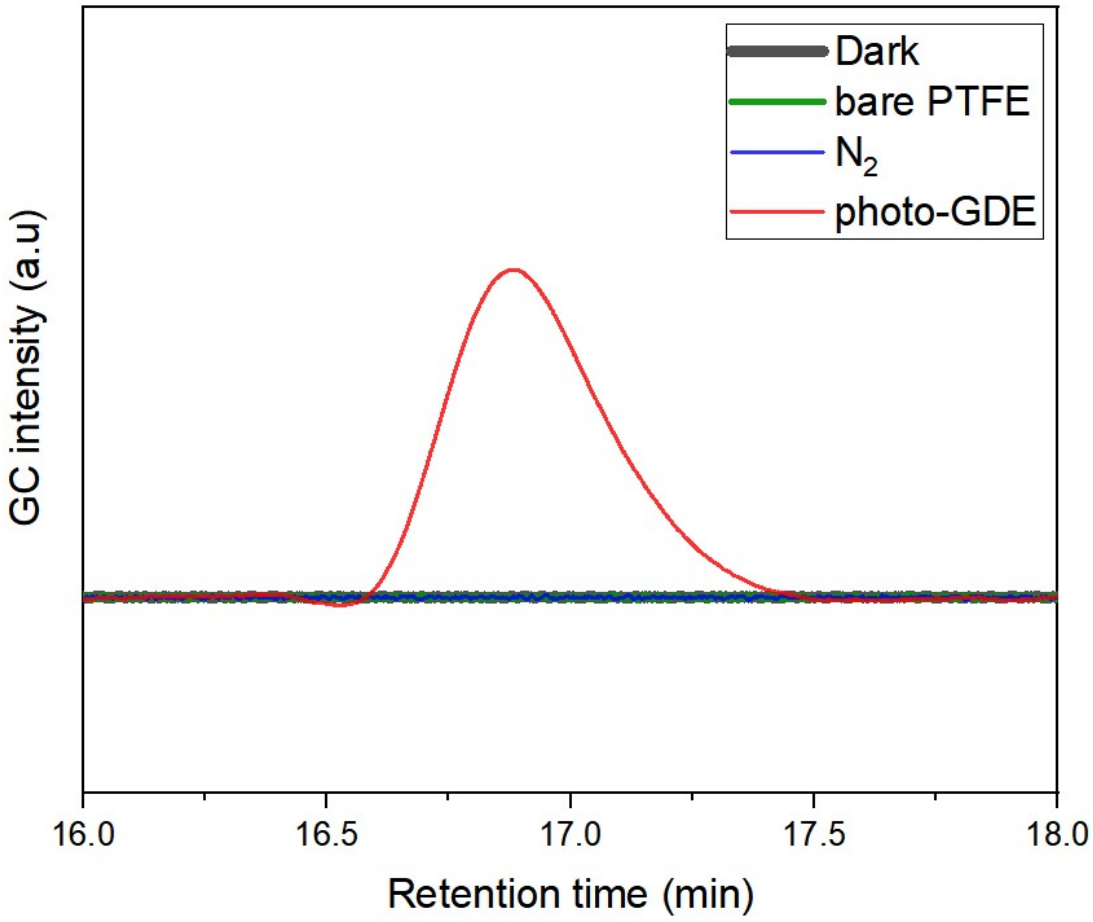

Figure S9. CO peak intensity from gas chromatography analysis under various reaction conditions. i) Without light irradiation (dark line), ii) with light irradiation of N_2 and H_2O streams in the absence of CO_2 (blue line), iii) with light irradiation in the presence of CO_2 using a bare PTFE film without photocatalysts (green line), and iv) with light irradiation in the presence of CO_2 with the P25 photocatalyst (red line).

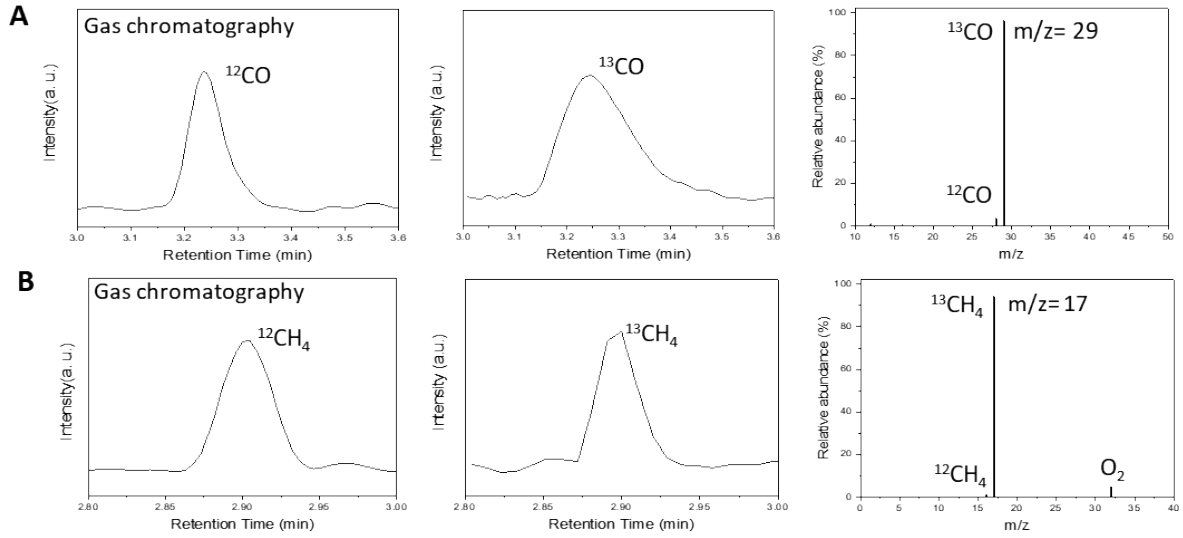

Figure S10. the isotope-labelling test. the GC–MS chromatogram and mass spectra of (**A**) CO and (**B**) CH_4.

Isotope-labeled carbon dioxide ($^{13}CO_2$) was subjected to photoreduction under the same reaction conditions, albeit at a low gas flow rate to obtain a high number of products beyond the detection limit of the MS detector. The MS signals for the two main products, *i.e.*, CO and CH_4, respectively, were investigated. In both products, most of the mass components mainly correspond to products containing ^{13}C. For CO, the ion chromatography peak appears at ~3.24 min, which corresponds to CO as the main product. On the other hand, in the case of general CO_2 photoreduction, the main MS signal observed at m/z = 28 corresponds to ^{12}CO, and in the case of the isotope-labeled reaction, the main MS signal observed at m/z = 29 corresponds to ^{13}CO. Thus, this confirms that the CO product originates from photoreduction of CO_2 in our flow reactor. Similarly, CH_4 from the flow reactor system is also a direct product of the photoreduction of CO_2, as its main MS signal at m/z = 17 corresponds to $^{13}CH_4$.

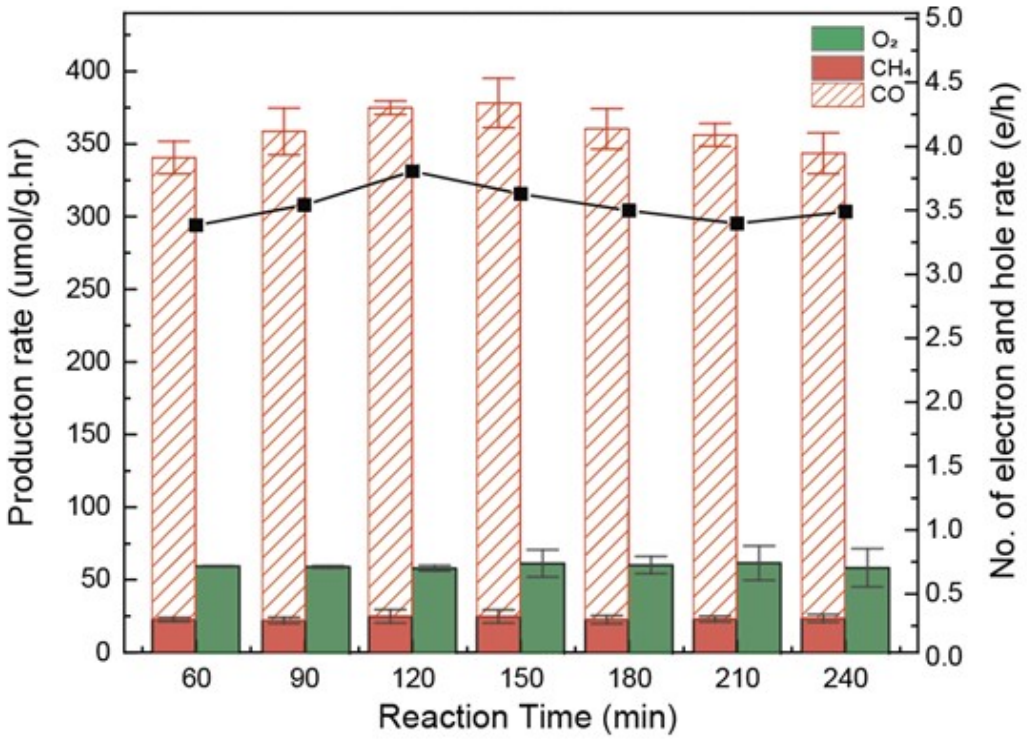

Figure S11. O_2 production rates compared with those of CO and CH_4 (left), and the number ratio of the generated electrons and holes (right). The reaction conditions were the same as those shown in Fig. 4.

In order to enhance our comprehension of the full cycle reaction in this system, O_2 production rate from water oxidation was measured. During a reaction time of 4 hours, the total production rate from CO_2R products was greater than ~350 μmol/g·h, while the production rate of O_2 from water oxidation was considerably lower (~60 μmol/g·h), reflecting the total number of electrons and holes used in the products. Generally, two electrons are needed to form CO, eight electrons to form CH_4, and four holes to form O_2. The ratio of the photogenerated holes to electrons (e/h ratio) is ≥3 during the reaction, which was unexpected given that only CO_2R and stoichiometric water oxidation were expected to occur during photocatalysis. When light energy is absorbed by the photocatalyst, one electron-hole pair is produced. According to the theory, the number of electrons and holes in the product should be equal (e/h rate = 1). It is important to highlight that other research studies have also observed an e/h ratio greater than 1 and that there is no consistent explanation for this phenomenon in the field. One relevant study [10] proposed various possible explanations, such as surface charge trapping, O_2 adsorption, and oxidation of Cl-contaminants. Interestingly, this study also found that the e/h ratio tended to approach unity after prolonged photocatalytic operation (up to 50 hours).

In our case, although the exact cause of this phenomenon remains unclear, based on the characteristics of our catalyst system observed during CO_2 reaction, it is possible to infer that the detected amount of O_2 decreased due to the rapid desorption of OH intermediates that facilitate the detachment of reaction products before O_2 formation. Consequently, the generated holes are expected to primarily oxidize water into OH and H_2O_2. We aim to investigate the specific and possibly limiting role of water oxidation in future research.

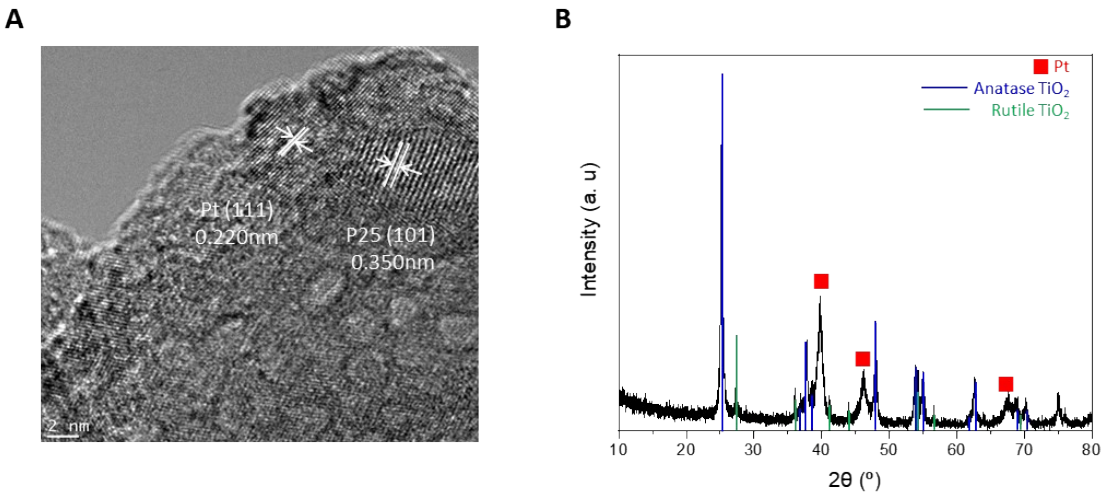

Figure S12. Characterizations of Pt-P25. (**A**) The as-synthesized Pt-P25 composite exhibits matching lattice distances for Pt (111) and P25 (101). (**B**) XRD data.

The lattice distance of Pt-P25 composite catalyst was measured by high-resolution transmission electron microscopy (HRTEM). The Pt-P25 exhibits matching lattice distance for Pt (111) [11]and P25 (101) [12] by transmission electron microscope (TEM). The peak positions of Pt [13] and P25, composed with anatase and rutile TiO_2 [14]was demonstrated by X-ray diffraction (XRD) analyses.

References and Notes

1. J. Taing, M. H. Cheng and J. C. Hemminger, *ACS Nano*, 2011, **5**, 6325–6333.
2. Y. Li, Y. Cai, X. Chen, X. Pan, M. Yang and Z. Yi, *RSC Adv*, 2016, **6**, 2760–2767.
3. S. Kumar, M. A. Isaacs, R. Trofimovaite, L. Durndell, C. M. A. Parlett, R. E. Douthwaite, B. Coulson, M. C. R. Cockett, K. Wilson and A. F. Lee, *Appl Catal B*, 2017, **209**, 394–404.
4. L. Wang, S. Duan, P. Jin, H. She, J. Huang, Z. Lei, T. Zhang and Q. Wang, *Appl Catal B*, 2018, **239**, 599–608.
5. H. M. Hwang, S. Oh, J. H. Shim, Y. M. Kim, A. Kim, D. Kim, J. Kim, S. Bak, Y. Cho, V. Q. Bui, T. A. Le and H. Lee, *ACS Appl Mater Interfaces*, 2019, **11**, 35693–35701.
6. M. Ye, X. Wang, E. Liu, J. Ye and D. Wang, *ChemSusChem*, 2018, **11**, 1606–1611.
7. Q. Chen, Y. Ma, B. Qi, T. Zhang, L. Wang, J. Shi and X. Lan, *Appl Surf Sci*, 2021, **555**, 149648.
8. Z. Wang, W. Zhou, X. Wang, X. Zhang, H. Chen, H. Hu, L. Liu, J. Ye and D. Wang, *Catalysts*, 2020, **10**, 1–11.
9. W. Jia, T. Liu, Q. Li and J. Yang, *Catal Today*, 2019, **335**, 221–227.
10. X. Zhu, A. Anzai, A. Yamamoto and H. Yoshida, *Appl Catal B*, 2019, **243**, 47–56.
11. L. Wang, R. Tang, A. Kheradmand, Y. Jiang, H. Wang, W. Yang, Z. Chen, X. Zhong, S. P. Ringer, X. Liao, W. Liang and J. Huang, *Appl Catal B*, 2021, **284**, 119759.
12. X. Zhao, J. Zhao, J. He, B. Li, Y. Zhang, J. Hu, H. Wang, D. Zhang and Q. Liu, *ACS Appl Energy Mater*, 2020, **3**, 6180–6187.
13. B. Abida, L. Chirchi, S. Baranton, T. W. Napporn, H. Kochkar, J. M. Léger and A. Ghorbel, *Appl Catal B*, 2011, **106**, 609–615.
14. Y. Jiao, H. Jiang and F. Chen, *ACS Catal*, 2014, **4**, 2249–2257.